

Trapped in action: direct visualization of DNA methyltransferase activity in living cells

Lothar Schermelleh¹, Fabio Spada¹, Hariharan P Easwaran², Kourosh Zolghadr¹, Jean B Margot², M Cristina Cardoso² & Heinrich Leonhardt^{1,2}

DNA methyltransferases have a central role in the complex regulatory network of epigenetic modifications controlling gene expression in mammalian cells. To study the regulation of DNA methylation in living cells, we developed a trapping assay using transiently expressed fluorescent DNA methyltransferase 1 (Dnmt1) fusions and mechanism-based inhibitors 5-azacytidine (5-aza-C) or 5-aza-2'-deoxycytidine (5-aza-dC). These nucleotide analogs are incorporated into the newly synthesized DNA at nuclear replication sites and cause irreversible immobilization, that is, trapping of Dnmt1 fusions at these sites. We measured trapping by either fluorescence bleaching assays or photoactivation of photoactivatable green fluorescent protein fused to Dnmt1 (paGFP-Dnmt1) in mouse and human cells; mutations affecting the catalytic center of Dnmt1 prevented trapping. This trapping assay monitors kinetic properties and activity-dependent immobilization of DNA methyltransferases in their native environment, and makes it possible to directly compare mutations and inhibitors that affect regulation and catalytic activity of DNA methyltransferases in single living cells.

np DNA methylation has a central role in the epigenetic control of mammalian gene expression during development and is required for X inactivation, genomic imprinting and silencing of retroviral elements^{1,2}. Until now, four DNA methyltransferases, Dnmt1, Dnmt2, Dnmt3a and Dnmt3b, are known in mammals, although the functional significance of the weak activity of Dnmt2 is still unclear^{3–7}. Dnmt3a and Dnmt3b are *de novo* methyltransferases implicated in setting up DNA methylation patterns during development¹. The major mammalian DNA methyltransferase, Dnmt1, maintains the methylation patterns after DNA replication and associates with the replication machinery during S phase⁸. Dnmt1 has been shown to interact with several different proteins including PCNA, HDACs, SUV39H1, HP1, MeCP2, DMAP1, E2F1, pRb and p53 (refs. 9–14). Changes in DNA methylation patterns, that is, general hypomethylation and local hypermethylation, are commonly found in cancerous cells¹⁵, and hypomethylation has been directly shown to cause genome instability and tumors in mice¹⁶. The regulatory mechanism(s) responsible for these methylation changes are still unknown. Notably, maintenance

of methylation patterns has been observed in the human HCT116 colorectal carcinoma cell line after inactivation of both *DNMT1* alleles, indicating possible differences in the regulation of DNA methylation in mouse and human or in transformed cells¹⁷.

The basic enzymatic mechanism of the methylation reaction has been worked out *in vitro* by biochemical studies with purified enzymes^{18,19}. The regulation of DNA methylation in mammalian cells, however, is still far from being understood, mostly owing to the fact that multiple methyltransferases are involved that interact with each other as well as with many nuclear factors. Moreover, the substrate itself, the cytosine residue, is embedded in highly dynamic and regulated chromatin structure. Here we describe a method to assay the activity of Dnmt1 in defined chromatin domains of single living cells. The method is based on the ability of Dnmt1 to form a stable covalent complex with the mechanism-based inhibitors 5-aza-C and 5-aza-dC upon their incorporation into DNA during replication. Trapping of GFP-Dnmt1 fusions is measured by fluorescence recovery after photobleaching (FRAP) analysis and reflects the enzymatic activity of the fusion protein. This assay can be used for studying the activity and targeting of Dnmt1 mutants, and for testing candidate catalytic inhibitors in living cells.

RESULTS

Rationale of the DNA methyltransferase trapping assay

To directly test the enzymatic activity of DNA methyltransferases in single living cells we developed an assay based on FRAP measurements in the presence of 5-aza-C and 5-aza-dC. The assay takes advantage of the transient covalent complex formation of the methyltransferase with the C6 position of the cytosine base ring to activate the C5 position for methyl group transfer^{20,21}. After methyl group transfer the enzyme is released from the complex by β elimination with the proton at the C5 position (**Fig. 1a**). The DNA methyltransferase inhibitors 5-aza-C and 5-aza-dC are widely used in research and clinical applications as demethylating drugs²². Both inhibitors are incorporated during DNA replication instead of cytosine residues throughout the genome including at potential methylation sites. The absence of the proton at the C5 position of the 5-aza analog prevents β elimination, the final step of the methylation reaction, leaving the methyltransferase trapped

¹Ludwig Maximilians University Munich, Department of Biology II, Großhaderner Str. 2, 82152 Planegg-Martinsried, Germany. ²Max Delbrueck Center for Molecular Medicine, FVK, Wiltbergstr. 50, 13125 Berlin, Germany. Correspondence should be addressed to H.L. (h.leonhardt@lmu.de).

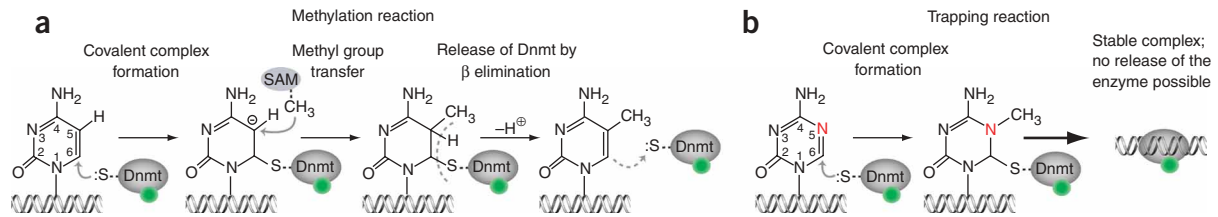


Figure 1 | Schematic representation of the DNA methylation reaction. **(a)** A covalent complex is formed between the sulfhydryl group of cysteine in the Pro-Cys motif of DNA methyltransferase (Dnmt) and the C6 position of cytosine base ring. Then a methyl group is transferred from *S*-adenosyl-L-methionine (SAM) followed by the release of the enzyme. **(b)** The absence of a proton at the N5 position of the 5-aza-C base ring prevents β elimination and thus causes trapping of the enzyme. Green dots represent GFP fused to the enzyme.

(Fig. 1b). Consequently, the free enzyme pool is depleted with progressing S phase, and existing methylation patterns cannot be maintained leading to global genome demethylation.

Direct visualization of DNA methyltransferase trapping

To visualize the distribution and mobility of Dnmt1 in living cells, we constructed a GFP-Dnmt1 fusion comprising the ubiquitously expressed long isoform of the mouse Dnmt1 tagged at the amino terminus with enhanced GFP²³. GFP-Dnmt1 is catalytically active as it is able to restore cytosine methylation levels when transiently expressed in mouse embryonic stem (ES) cells deficient of Dnmt1 (Supplementary Fig. 1 online). Coexpression in mouse myoblast cells of GFP-Dnmt1 and proliferating cell nuclear antigen (PCNA)

fused to red fluorescent protein (RFP-PCNA) that labels sites of DNA replication²⁴ showed that the GFP-Dnmt1 localizes at S phase replication foci just like endogenous Dnmt1 (Fig. 2a and ref. 23). After bleaching of single or multiple replication foci, we observed nearly complete recovery of the GFP signal within about 90 s indicating a rapid recruitment of new, fluorescent Dnmt1 fusion proteins at these sites. In contrast, the recovery of RFP-PCNA fluorescence was much slower, and the partial recovery after several minutes is likely to be caused by a *de novo* assembly of the trimeric PCNA ring at adjacent replication sites rather than by a constant protein exchange²⁵. After the incubation with 5-aza-C, however, we observed no recovery of GFP-Dnmt1 fluorescence at bleached replication foci (Fig. 2b) reflecting the depletion of the mobile fraction caused by trapping of the active fusion protein at the newly synthesized DNA. This is consistent with the observation that after incubation with 5-aza-C GFP-Dnmt1 no longer colocalized with RFP-PCNA but seemed to be retained at earlier, adjacent replication sites. These results demonstrate a 5-aza-C-dependent immobilization of GFP-Dnmt1 at sites of DNA replication.

Enzyme trapping depends on catalytic activity

Because 5-aza-C is a mechanism-based inhibitor, immobilization of the GFP-Dnmt1

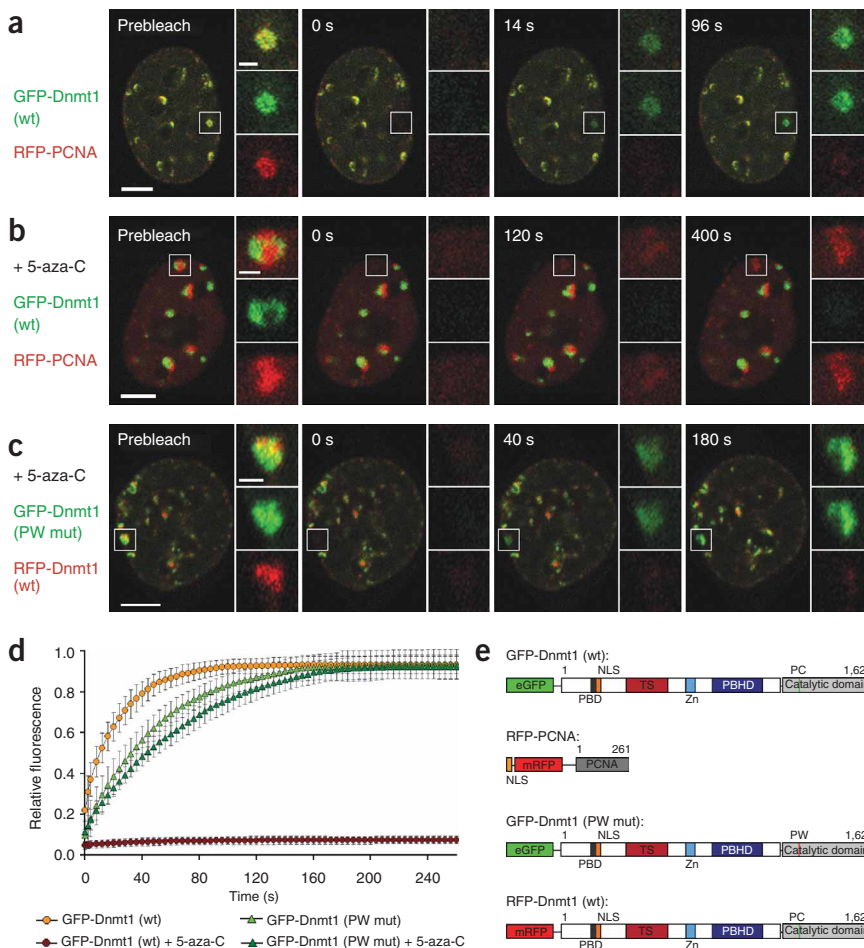


Figure 2 | Trapping of active Dnmt1 after 5-aza-C treatment. **(a)** FRAP of GFP-Dnmt1 and RFP-PCNA coexpressed in mouse myoblasts without drug treatment. Late S phase nucleus with GFP-Dnmt1 (green) and RFP-PCNA (red) largely colocalize at replication sites. Inset shows the replication focus. **(b)** Analogous experiment after treatment with 300 μ M 5-aza-C for 2 h. **(c)** Comparative FRAP of wild-type RFP-Dnmt1 and the GFP-Dnmt1 PW mutant after treatment with 300 μ M 5-aza-C for 2 h. Bars in **a–c** represent 5 μ m (1 μ m in insets). **(d)** Quantitative evaluation of FRAP data showing mean curves. Error bars represent standard deviations. For comparison, only late S phase nuclei were evaluated. **(e)** Schematic representation of the fusion proteins. PBD, PCNA binding domain; NLS, nuclear localization sequence; TS, targeting sequence; Zn, Zn-binding domain; PBHD, poly(bromo) homology domain.

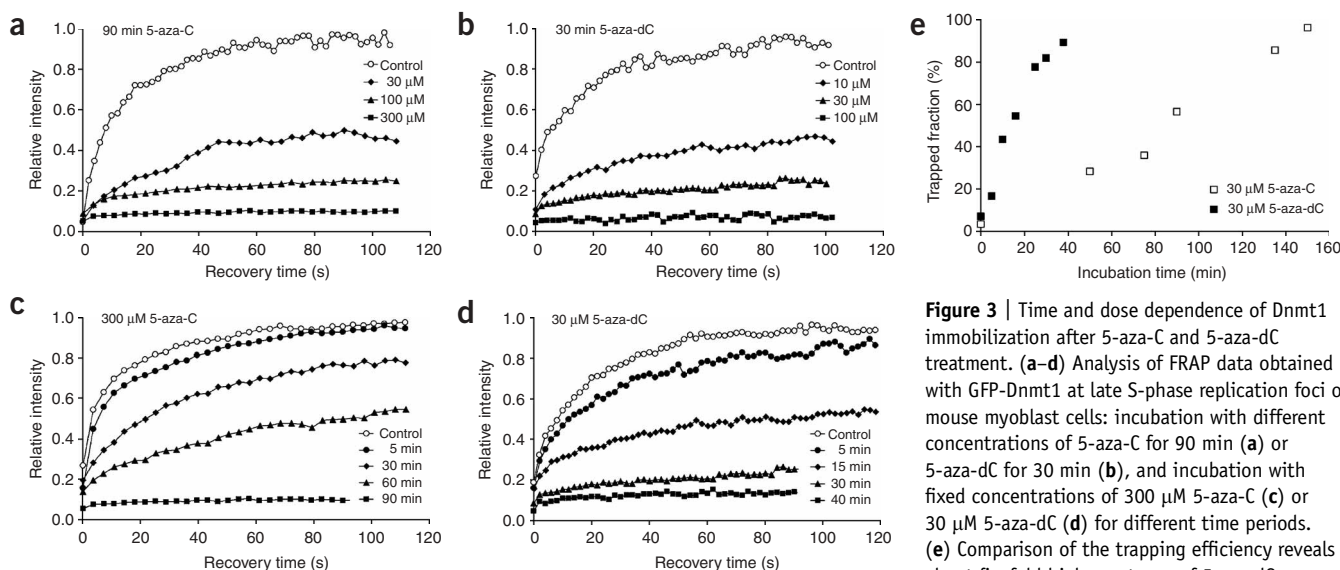


Figure 3 | Time and dose dependence of Dnmt1 immobilization after 5-aza-C and 5-aza-dC treatment. **(a–d)** Analysis of FRAP data obtained with GFP-Dnmt1 at late S-phase replication foci of mouse myoblast cells: incubation with different concentrations of 5-aza-C for 90 min **(a)** or 5-aza-dC for 30 min **(b)**, and incubation with fixed concentrations of 300 μM 5-aza-C **(c)** or 30 μM 5-aza-dC **(d)** for different time periods. **(e)** Comparison of the trapping efficiency reveals about fivefold higher potency of 5-aza-dC over 5-aza-C, reflecting the higher incorporation rate of the deoxy variant.

fusion should be a direct measure of methyltransferase activity. To directly test this, we introduced a site-specific mutation inactivating the catalytic center of Dnmt1. We mutated the conserved Pro-Cys motif, which is involved in the covalent complex formation²¹, by exchanging the cysteine for a tryptophan (Dnmt1 C1229W, here referred to as PW mutant). For direct comparison we generated an RFP-tagged wild-type Dnmt1 and cotransfected cells with the wild-type and mutant construct. Both fusion proteins localized at replication foci in S-phase cells as observed for the native protein. In sharp contrast to the wild-type Dnmt1 fusion, the PW mutant did still recover after photobleaching even after 2 h of incubation with 300 μM 5-aza-C (**Fig. 2c**). This indicates that the mutant protein does not form a covalent complex with the DNA, which is consistent with earlier biochemical studies on bacterial DNA (cytosine-5) methyltransferases²⁶. In control experiments without 5-aza-C treatment, we determined a mobile fraction of ~90% for both, wild-type Dnmt1 and PW mutant (**Fig. 2d**). After 90–120 min incubation with 5-aza-C, however, the mobile fraction of the active wild-type fusion dropped to ~5%, whereas the mobility of the PW mutant was not affected. Half-times of recovery ($t_{1/2}$) were 15 s and 34 s for wild type and PW mutant, respectively, without 5-aza-C treatment, and 40 s for the PW mutant after 5-aza-C treatment (300 μM, 120 min). The slower recovery of the PW mutant as compared to the wild-type fusion in untreated cells may be due to altered dissociation kinetics of the mutant. The decelerated recovery of the PW mutant in the presence of 5-aza-C is likely due to a general slowdown of the replication and methylation machinery caused by trapping of the endogenous Dnmt1 protein. The fusion proteins are schematically represented in **Figure 2e**. Taken together, the catalytic activity of a Dnmt1 fusion construct can be directly assayed as covalent complex formation rate by FRAP in the presence of 5-aza-C.

Trapping rate is inhibitor-, dose- and time-dependent

To evaluate the trapping assay we compared different incubation times and concentrations of the two widely used demethylating

drugs 5-aza-C and 5-aza-dC (**Fig. 3**). In comparison, 5-aza-dC was more potent than 5-aza-C in depleting the nucleoplasmic pool of GFP-Dnmt1. About threefold lower concentrations and threefold shorter incubation times were sufficient to reach the same levels of depletion with 5-aza-dC as compared to 5-aza-C (**Fig. 3a,b**). With longer incubation times the nucleoplasmic GFP-Dnmt1 pool became progressively immobilized in cells treated with 300 μM 5-aza-C or 30 μM 5-aza-dC, until complete depletion was reached after about 90 min or 40 min, respectively (**Fig. 3c,d** and **Supplementary Video 1** online). Direct comparison of the same concentration of the two inhibitors showed that 5-aza-dC is about fivefold more potent than 5-aza-C in depleting the nucleoplasmic pool of GFP-Dnmt1 (**Fig. 3e**). This is consistent with the fact that 5-aza-dC is directly incorporated into DNA, whereas 5-aza-C has to be modified before incorporation and can also be incorporated into RNA^{27,28}. These results demonstrate that the assay is sensitive to the type of inhibitor, its dose and incubation time.

Experiments with human DNMT1 fused to GFP expressed in human neuroblastoma cells also showed trapping of the fusion protein upon treatment with 5-aza-dC, thus demonstrating the general applicability of the trapping assay not only in mouse but also in human cells (**Supplementary Fig. 2** online).

Direct visualization of trapping with paGFP-Dnmt1

For further dynamic studies we fused Dnmt1 to photoactivatable GFP (paGFP-Dnmt1) and coexpressed with RFP-PCNA to mark replication sites. Photoactivatable GFP has a low initial absorbance at 488 nm, which increases ~100-fold by photoconversion after excitation with ~400-nm light²⁹. Photoactivation of paGFP-Dnmt1 at replication sites in an untreated control cell revealed rapid dissociation of paGFP-Dnmt1 (**Fig. 4a**). Upon treatment with 5-aza-dC we observed no dissociation of paGFP-Dnmt1, directly showing the trapping of the enzyme (**Fig. 4b**). In contrast, local activation of paGFP-Dnmt1 in a G1 nucleus was followed by a quick redistribution throughout the entire nucleus as no incorporation of 5-aza-dC can take place at this cell cycle stage (**Fig. 4c**).

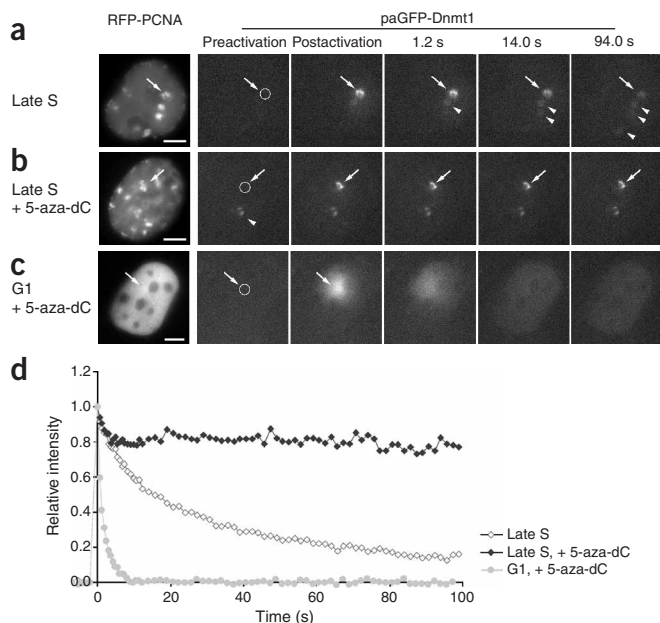


Figure 4 | Direct visualization of trapping by photoactivation of paGFP-Dnmt1. (**a–c**) Mouse myoblast cells were cotransfected with RFP-PCNA to identify cell cycle stage and replication sites of S-phase cells. Photoactivated paGFP-Dnmt1 dissociates from the irradiated site (indicated by arrows) and associates with neighboring replication sites (indicated by arrowheads) until a new equilibrium is reached (94 s; **a**). Upon treatment with 30 μ M 5-aza-dC for 1 h, no dissociation of paGFP-Dnmt1 is observed (arrow; **b**). The arrowhead indicates a replication focus irradiated a few minutes earlier. Note that fluorescence intensity of trapped paGFP-Dnmt1 at this site also does not change during the time course. Local activation of paGFP-Dnmt1 (arrow) in a G1 nucleus is followed by a quick redistribution throughout the entire nucleus, as no incorporation of 5-aza-dC can take place in this cell cycle stage (**c**). (**d**) Quantitative evaluation of the fluorescence activation experiments shown in **a–c**.

These fundamental differences in Dnmt1 dissociation kinetics are underscored by the quantitative evaluation (**Fig. 4d**). Without treatment paGFP-Dnmt1 dissociates with a $t_{1/2}$ of ~ 12 s to reach a level of $\sim 15\%$ at the end of the observation period. After 5-aza-dC treatment fluorescence levels drop to $\sim 80\%$ of the initial fluorescence and then remain constant during the rest of the observation period. In G1 nuclei, paGFP-Dnmt1 shows a very rapid dissociation to 0% with a $t_{1/2}$ of ~ 0.5 s. This application of paGFP is the first direct demonstration of the action of mechanism-based inhibitors and covalent complex formation with DNA methyltransferases in living cells.

DISCUSSION

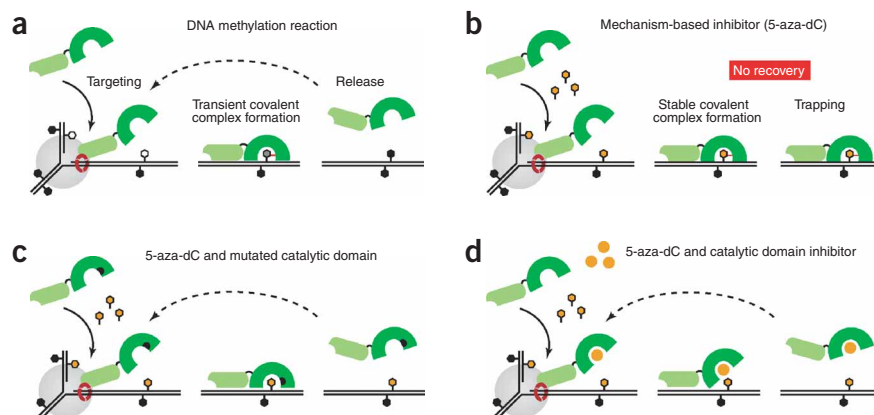
We owe most of our basic knowledge about DNA methylation to classical biochemical approaches, which cannot reproduce the complexity of living, mammalian cells. Recent biochemical studies of DNA methyltransferase activity involved detection of either

lowered DNA methyltransferase levels in nuclear extracts^{30,31} or of elevated levels of DNA methyltransferase–DNA adducts in genomic DNA extracts after 5-aza-dC treatment in both cases by immunoblotting analysis³². The trapping assay described here makes it possible for the first time to study Dnmt1 in its natural environment with its natural substrate in the context of dynamic chromatin structures and simultaneously ongoing DNA replication. Both activity and subnuclear targeting of DNA methyltransferases can be analyzed *in situ* at different cell cycle stages in single living cells.

The basic principle of the trapping assay and its application to test catalytic mutants and potential inhibitors of the catalytic domain is illustrated in **Figure 5**. The method takes advantage of the covalent complex formation of DNA methyltransferases with cytosine residues during catalysis. By using a catalytic mutant of Dnmt1 we show that trapping depends on catalytic activity, providing direct evidence that the technique can be used to monitor DNA methyltransferases actively engaged in the methylation reaction. Comparing different concentrations and incubation times of known DNA methyltransferase inhibitors, 5-aza-C and 5-aza-dC, we demonstrate the sensitivity of this assay.

The assay can be applied to all DNA (cytosine-5) methyltransferases that form a covalent complex with cytosine residues and have a mobile nuclear distribution. Here we focus on Dnmt1 as it is of major clinical relevance. Unlike *de novo* methyltransferases, Dnmt1 is ubiquitously expressed in proliferating cells in which it

Figure 5 | Postreplicative action of Dnmt1 and rationale of the trapping assay. (**a**) Regulatory and catalytic domains of Dnmt1 are in lighter and darker shades of green, respectively. For simplicity only events at the leading strand are shown. Methylated and nonmethylated cytosines are depicted as black and white hexagons, respectively. The trimeric PCNA ring (red) is shown as part of the replication complex (grey circle). Dnmt1 transiently interacts with PCNA at the replication site, binds to CpG sites and forms a transient covalent complex with the cytosine residue (red line). After methyl group transfer the enzyme is released and becomes available for another round of methylation (dotted arrow). (**b**) Mechanism-based inhibitors (orange hexagons) are incorporated into DNA during S phase. Dnmt1 forms a stable complex with these inhibitors and becomes trapped. (**c**) In contrast, trapping is eliminated if the catalytic domain of Dnmt1 is mutated (black dot). (**d**) Likewise, blocking the catalytic site of Dnmt1 with new types of small-molecule inhibitors (filled orange circles) would prevent covalent complex formation.



maintains normal as well as aberrant methylation patterns through DNA replication. In cancer cells tumor-suppressor genes are frequently silenced by methylation. Thus, pharmaceutical strategies aim at transient inhibition of Dnmt1 to reactivate such epigenetically silenced genes and re-establish normal cell cycle and growth control²². Mechanism-based inhibitors presently under clinical trials, however, generate Dnmt1-DNA adducts that may lead to cytotoxic effects³³. Therefore, small-molecule inhibitors targeting the catalytic domain of Dnmt1 are actively sought after, and candidate molecules can now be directly tested by their ability to prevent 5-aza-dC-mediated trapping of GFP-Dnmt1 (Fig. 5d). It should be noted that some compounds may affect cell cycle progression or DNA replication, which would reduce the incorporation of 5-aza-dC and thus indirectly prevent trapping of DNA methyltransferases. Such unspecific cell cycle progression effects can, however, be identified using the changing subnuclear GFP-Dnmt1 and RFP-PCNA patterns to monitor cell cycle progression^{23,34}. In any case, newly identified compounds need to be further characterized *in vitro* with additional biochemical DNA methyltransferase activity assays.

In summary, the mechanism-based trapping assay provides a new approach to directly study the regulation of DNA methylation and to test the effect of mutations and interacting factors in living cells. In addition, this method now makes it possible to directly investigate the cellular effects of demethylating drugs like 5-aza-dC that are widely used in basic research and in cancer therapy and offers an approach to test new types of DNA methyltransferase inhibitors.

METHODS

Cell culture and transfections. We cultured mouse C2C12 myoblast cells in DMEM containing 25 mM HEPES and supplemented with 20% fetal calf serum and 50 µg/ml gentamycin. We grew cells to 30–40% confluence on Lab-Tek chamber slides (Nunc) and then cotransfected them with the indicated expression constructs by standard Ca₂PO₄ DNA coprecipitation followed by a glycerol shock³⁵, or using TransFectin transfection reagent (Bio-Rad) according to the manufacturer's instructions. We then incubated cells overnight before performing drug treatment and live-cell analysis. For culture, transfection and 5-methylcytosine staining of mouse ES and human cell lines, see **Supplementary Methods** online.

Expression constructs. We visualized replication sites using a red fluorescent fusion with full-length human PCNA (RFP-PCNA)³⁶. To generate GFP-Dnmt1 (previously referred to as GMT1L) we cloned the full-length mouse cDNA of the long Dnmt1 isoform in the pEGFP-C1 vector (Clontech)²³. To generate RFP-Dnmt1 and paGFP-Dnmt1 we replaced the sequence encoding GFP with those encoding mRFP1³⁷ and paGFP²⁹, respectively. We introduced the C1229W mutation (PW mutant) into the Dnmt1 cDNA by site-directed mutagenesis (QuikChange Kit, Stratagene) and confirmed it by DNA sequencing. We tested all fusion constructs by expression in COS-7 or 293T cells and subsequent western blot analysis³⁴.

Live-cell microscopy, FRAP analysis and photoactivation. We added 5-Aza-C or 5-aza-dC (Sigma) at indicated final concentrations and incubated cells as indicated before starting live-cell observations. We performed FRAP experiments using a Zeiss LSM 510 confocal laser scanning microscope with a 63×, 1.4 NA Plan-Apochromat oil immersion objective. We excited

fluorophores with a 488-nm Ar laser and a 543-nm HeNe laser. We typically recorded confocal image series with a frame size of 256 × 256 pixels and a pixel size of 70–90 nm. The laser power was typically set to 1–5% transmission with the pinhole opened to 2 Airy units. For FRAP analysis, we selected a region of interest and photobleached it by an intense 488-nm Ar laser beam (laser set to maximum power at 100% transmission) for 1 s. Before and after bleaching, we recorded confocal image series at 2–5 s intervals (typically 6 prebleach and 50–100 postbleach frames). Mean fluorescence intensities of the bleached region were corrected for background and for total nuclear loss of fluorescence over the time course, and normalized to the mean of the last 4 prebleach values. For the quantitative evaluation of FRAP experiments, we averaged data of 4–6 nuclei, calculated the mean curve as well as the standard deviation and displayed these using GraphPad Prism 4.01 software. We calculated the $t_{1/2}$ of recovery from the average curves.

We performed photoactivation experiments using a DeltaVision widefield epifluorescence microscope system (Applied Precision) equipped with a 60×, 1.4 NA Plan-Apochromat objective and appropriate filter sets. Photoactivatable GFP was activated using a 405 nm diode laser coupled into the light path of the microscope. After laser photoactivation for 1 s (100% transmission), we acquired epifluorescence time series at 0.6-s intervals. For quantitative evaluation, we corrected the mean fluorescence intensities of the activated area for background and for the increase of fluorescence in a nonirradiated nuclear control region, and then normalized it to the value of the first time point after activation.

Note: Supplementary information is available on the Nature Methods website.

ACKNOWLEDGMENTS

We thank R.Y. Tsien for providing mRFP1 cDNA, J. Lippincott-Schwartz for providing paGFP cDNA, E. Li for mutant *Dnmt1* ES cells and P. Vertino for the human *DNMT1* cDNA. We thank M. Grohmann for sharing expression constructs. We are grateful to I. Grunewald and A. Gahl for technical assistance. This work was supported by grants from the Deutsche Forschungsgemeinschaft and the Max Delbrück Center to H.L. and M.C.C.

COMPETING INTERESTS STATEMENT

The authors declare that they have no competing financial interests.

Published online at <http://www.nature.com/naturemethods/>
Reprints and permissions information is available online at
<http://npg.nature.com/reprintsandpermissions/>

- Li, E. Chromatin modification and epigenetic reprogramming in mammalian development. *Nat. Rev. Genet.* **3**, 662–673 (2002).
- Jaenisch, R. & Bird, A. Epigenetic regulation of gene expression: how the genome integrates intrinsic and environmental signals. *Nat. Genet.* **33** (Suppl.), 245–254 (2003).
- Bestor, T.H. The DNA methyltransferases of mammals. *Hum. Mol. Genet.* **9**, 2395–2402 (2000).
- Robertson, K.D. DNA methylation and chromatin—unraveling the tangled web. *Oncogene* **21**, 5361–5379 (2002).
- Tang, L.Y. *et al.* The eukaryotic *DNMT2* genes encode a new class of cytosine-5 DNA methyltransferases. *J. Biol. Chem.* **278**, 33613–33616 (2003).
- Hermann, A., Schmitt, S. & Jeltsch, A. The human Dnmt2 has residual DNA-(cytosine-C5) methyltransferase activity. *J. Biol. Chem.* **278**, 31717–31721 (2003).
- Kunert, N., Marhold, J., Stanke, J., Stach, D. & Lyko, F.A. Dnmt2-like protein mediates DNA methylation in *Drosophila*. *Development* **130**, 5083–5090 (2003).
- Leonhardt, H., Page, A.W., Weier, H.U. & Bestor, T.H. A targeting sequence directs DNA methyltransferase to sites of DNA replication in mammalian nuclei. *Cell* **71**, 865–873 (1992).
- Chuang, L.S. *et al.* Human DNA-(cytosine-5) methyltransferase-PCNA complex as a target for p21WAF1. *Science* **277**, 1996–2000 (1997).

10. Rountree, M.R., Bachman, K.E. & Baylin, S.B. DNMT1 binds HDAC2 and a new co-repressor, DMAP1, to form a complex at replication foci. *Nat. Genet.* **25**, 269–277 (2000).
11. Robertson, K.D. *et al.* DNMT1 forms a complex with Rb, E2F1 and HDAC1 and represses transcription from E2F-responsive promoters. *Nat. Genet.* **25**, 338–342 (2000).
12. Fuks, F., Hurd, P.J., Deplus, R. & Kouzarides, T. The DNA methyltransferases associate with HP1 and the SUV39H1 histone methyltransferase. *Nucleic Acids Res.* **31**, 2305–2312 (2003).
13. Kimura, H. & Shiota, K. Methyl-CpG-binding protein, MeCP2, is a target molecule for maintenance DNA methyltransferase, Dnmt1. *J. Biol. Chem.* **278**, 4806–4812 (2003).
14. Esteve, P.O., Chin, H.G. & Pradhan, S. Human maintenance DNA (cytosine-5)-methyltransferase and p53 modulate expression of p53-repressed promoters. *Proc. Natl. Acad. Sci. USA* **102**, 1000–1005 (2005).
15. Jones, P.A. & Baylin, S.B. The fundamental role of epigenetic events in cancer. *Nat. Rev. Genet.* **3**, 415–428 (2002).
16. Gaudet, F. *et al.* Induction of tumors in mice by genomic hypomethylation. *Science* **300**, 489–492 (2003).
17. Rhee, I. *et al.* CpG methylation is maintained in human cancer cells lacking DNMT1. *Nature* **404**, 1003–1007 (2000).
18. Cheng, X. & Roberts, R.J. AdoMet-dependent methylation, DNA methyltransferases and base flipping. *Nucleic Acids Res.* **29**, 3784–3795 (2001).
19. Bestor, T.H. & Verdine, G.L. DNA methyltransferases. *Curr. Opin. Cell Biol.* **6**, 380–389 (1994).
20. Santi, D.V., Garrett, C.E. & Barr, P.J. On the mechanism of inhibition of DNA-cytosine methyltransferases by cytosine analogs. *Cell* **33**, 9–10 (1983).
21. Chen, L. *et al.* Direct identification of the active-site nucleophile in a DNA (cytosine-5)-methyltransferase. *Biochemistry* **30**, 11018–11025 (1991).
22. Christman, J.K. 5-Azacytidine and 5-aza-2'-deoxycytidine as inhibitors of DNA methylation: mechanistic studies and their implications for cancer therapy. *Oncogene* **21**, 5483–5495 (2002).
23. Easwaran, H.P., Schermelleh, L., Leonhardt, H. & Cardoso, M.C. Replication-independent chromatin loading of Dnmt1 during G2 and M phases. *EMBO Rep.* **5**, 1181–1186 (2004).
24. Leonhardt, H. *et al.* Dynamics of DNA replication factories in living cells. *J. Cell Biol.* **149**, 271–280 (2000).
25. Sporbert, A., Gahl, A., Ankerhold, R., Leonhardt, H. & Cardoso, M.C. DNA polymerase clamp shows little turnover at established replication sites but sequential *de novo* assembly at adjacent origin clusters. *Mol. Cell* **10**, 1355–1365 (2002).
26. Wyszynski, M.W., Gabbara, S. & Bhagwat, A.S. Substitutions of a cysteine conserved among DNA cytosine methylases result in a variety of phenotypes. *Nucleic Acids Res.* **20**, 319–326 (1992).
27. Jones, P.A. & Taylor, S.M. Cellular differentiation, cytidine analogs and DNA methylation. *Cell* **20**, 85–93 (1980).
28. Cihak, A. Biological effects of 5-azacytidine in eukaryotes. *Oncology* **30**, 405–422 (1974).
29. Patterson, G.H. & Lippincott-Schwartz, J. A photoactivatable GFP for selective photolabeling of proteins and cells. *Science* **297**, 1873–1877 (2002).
30. Robert, M.F. *et al.* DNMT1 is required to maintain CpG methylation and aberrant gene silencing in human cancer cells. *Nat. Genet.* **33**, 61–65 (2003).
31. Weisenberger, D.J. *et al.* Role of the DNA methyltransferase variant DNMT3b3 in DNA methylation. *Mol. Cancer Res.* **2**, 62–72 (2004).
32. Liu, K., Wang, Y.F., Cantemir, C. & Muller, M.T. Endogenous assays of DNA methyltransferases: Evidence for differential activities of DNMT1, DNMT2, and DNMT3 in mammalian cells *in vivo*. *Mol. Cell. Biol.* **23**, 2709–2719 (2003).
33. Juttermann, R., Li, E. & Jaenisch, R. Toxicity of 5-aza-2'-deoxycytidine to mammalian cells is mediated primarily by covalent trapping of DNA methyltransferase rather than DNA demethylation. *Proc. Natl. Acad. Sci. USA* **91**, 11797–11801 (1994).
34. Easwaran, H.P., Leonhardt, H. & Cardoso, M.C. Cell cycle markers for live cell analyses. *Cell Cycle* **4**, 453–455 (2005).
35. Cardoso, M.C. *et al.* Mapping and use of a sequence that targets DNA ligase I to sites of DNA replication *in vivo*. *J. Cell Biol.* **139**, 579–587 (1997).
36. Sporbert, A., Domaing, P., Leonhardt, H. & Cardoso, M.C. PCNA acts as a stationary loading platform for transiently interacting Okazaki fragment maturation proteins. *Nucleic Acids Res.* **33**, 3521–3528 (2005).
37. Campbell, R.E. *et al.* A monomeric red fluorescent protein. *Proc. Natl. Acad. Sci. USA* **99**, 7877–7882 (2002).